Cross-sectional Study

Optical coherence tomography angiography features of macular neovascularization in wet age-related macular degeneration: A cross-sectional study

Mahjoub Ahmed, Ben Mrad Syrine [*], Ben Abdesslem Nadia, Mahjoub Anis, Zinelabidine Karim, Ghorbel Mohamed, Mahjoub Hachemi, Krifa Fethi, Knani Leila

Ophthalmology Department, Farhat Hached's Hospital of Sousse, Tunisia

ABSTRACT

Background: OCT-A is a recent imaging technique allowing a non-invasive assessment of the retinal and choroidal microvasculature, providing valuable data for the diagnosis and monitoring of wet AMD. We aim to determine the diagnosis accuracy, describe the morphological features, and assess the clinical activity of MNV in wet AMD using OCT-A.

Materials and methods: We conducted a descriptive cross-sectional study over a 15-month period. We enrolled patients with treatment-naive and treated MNV secondary to wet AMD. Macular OCT-A images were obtained using a swept-source OCT-A device (Triton SS-OCT, Topcon, Tokyo, Japan). Morphologic characteristics and semi-automated measurements were analyzed on the en face projection OCT-Angiograms. For the qualitative analysis, determined the sensitivity of detection of the MNV using OCTA. When detected, we described its shape, branching pattern, anastomoses and loops, and vessel termination. We looked for the halo sign and the feeder vessel. We then defined the lesion's "pattern" reflecting its exudative activity. For the quantitative analysis, we measured the lesion's area in square millimeters, when its borders were clearly defined.

Results: 70 eyes from 55 patients were enrolled in this study. Type 1 MNV was identified in 57,1% eyes, type 2 in 21,4%, mixed type 1 and2 in 1,4%, type 3 in 1,4% and unclassified fibrotic MNV in 18,6%. 55,7% were active and 44,3% were inactive. Sensitivity of detection was 85% for type 1 lesions, 100% for type 2, mixed and type 3 lesions, and 92% for unclassified fibrotic lesions. It was 84,6% for active lesions and 96,8% for inactive lesions. For each detected lesion, shape was well-defined (medusa, glomerulus, seafan), long liner vessels or ill-defined. Branching pattern was dense or loose. Anastomoses and vascular loops were numerous or few. Termination was in an anastomotic arcade or in a dead-tree aspect. Halo sign was present or absent and feeder vessel was detected or not. All types combined, 41,3% of the lesions were "pattern I" and 58,7% were pattern II. We reported a correlation rate of 84,8% between the lesion's activity on MI and « pattern I » on OCT-A, and of 96,6% between absence of activity signs on MI and « pattern II » on OCT-A The mean area of inactive lesions was slightly larger than that of active lesions with respective values of 3.86 mm^2 and 2.92 mm^2

Conclusion: OCT-A is a non-invasive, safe, and reproducible retinal imaging technique with a high sensitivity of detection of MNV in AMD. It provides useful qualitative and quantitative data. The involvement of OCT-A in the treatment decision for MNV in AMD is linked to identifying the "pattern" of the lesion reflecting its active or inactive status.

1. Introduction

Age related macular degeneration (AMD) is a progressive degenerative retinal disease affecting the macula. It affects 7–8% of the world population and represents the first cause of central vision loss in individuals aged 50 or more in developed countries [1]. In 2040, this condition would affect around 288 million people worldwide [2]. Clinically, we differentiate two stages of the disease: the early stage "early AMD" and the advanced stage "Late AMD" marked by deterioration of visual acuity. At this stage, we also distinguish the exudative

form or neovascular AMD and the non-exudative form or atrophic AMD [3]. The exudative form is characterized by a rapid course with a significant risk of vision loss after a few months. Retinal fluorescein angiography (FA) has long been considered the gold standard for the diagnosis, classification and monitoring of AMD [4]. Indocyanine green angiography (ICGA) allows for a better analysis of structures below the retinal pigment epithelium (RPE) [5]. Recently, the diagnostic approach of macular pathologies has been revolutionized by the introduction of optical coherence tomography (OCT), particularly Spectral Domain OCT (SD-OCT). More recently in 2012, OCT angiography (OCT-A) was introduced by Jia et al. [6]. This high-resolution and non-invasive imaging technique allows a three-dimensional analysis of the retinal and choroidal microvasculature, providing valuable qualitative and quantitative data for the diagnosis and monitoring of numerous retinal pathologies, particularly AMD [7]. While the acquisition can sometimes be technically tricky, OCT-A remains a fast, reproducible, and safe technique for the patient.

Our study aims to determine the diagnosis accuracy, describe the morphological features and assess the clinical activity of macular neovascularization (MNV) in wet AMD using OCT-A.

2. Methods

2.1. Study type and population

We conducted a descriptive cross-sectional study over a 15-month period from March 2019 to June 2020, in the ophthalmology department of Farhat Hached hospital, Sousse, Tunisia. Our study is fully compliant with the STROCSS criteria [8], and is registered under the Unique Identifying Number UIN "researchregistry7027" https://www.researchregistry.com/browse-the-registry#home/registrationdetails/610ad5ccc99ae6001e46fb7f/. Patients with treatment-naive and treated MNV secondary to wet AMD were enrolled in this study. The diagnosis of wet AMD was based on the clinical presentation and multimodal imaging (MI), including structural OCT and FA when needed. We excluded eyes with early-AMD corresponding to the presence of soft drusen and retinal pigment epithelium alterations without macular neovascularization. The presence of any coexisting ocular condition affecting the macular region was also an exclusion criterion. Clinical data were collected from patient's interrogation specifying the age, gender and history of any previous intravitreal anti-vascular endothelial growth factor (VEGF) injections. All patients then underwent complete ophthalmic examination including best corrected visual acuity (BCVA), intra-ocular pressure (IOP) measurement, slit-lamp anterior segment examination and funduscopy.

Structural OCT imaging was performed using a swept-source OCT device (Triton SS-OCT, Topcon, Tokyo, Japan). It allowed us to identify the MNV and to determine its type, to visualize any subretinal fibrosis, to assess the presence of exsudative signs defining the lesion's clinical activity (Intraretinal and subretinal fluid) and to detect any degenerative lesions (intraretinal cysts and outer retinal tubulations ORTs). Presence of pigment epithelial detachment (PED), subretinal hyper-reflective material, intra-retinal hyper-reflective dots and evidence of outer retinal atrophy were also analyzed. We used the 2020's consensual nomenclature to report structural OCT features of wet AMD [9]. We used the term « unclassified fibrotic MNV » to designate fibrovascular lesions of unknown type.

2.2. OCT-A data acquisition

OCT-A imaging was performed using the same swept-source OCT device (Triton SS-OCT, Topcon, Tokyo, Japan) with a light source of 1050 nm and an A-scan rate of 100,000 scans per second. 6 × 6mm cube scans using automated layer segmentation were acquired for each eye. SMARTTrack system helped to reduce motion artifacts.

2.3. OCT-A data analysis

2.3.1. Qualitative analysis

As part of the qualitative analysis, we first looked at the sensitivity of detection of the MNV using OCTA. When detected on the en face OCT-A images, we described its morphologic shape: well-defined (medusa, glomerulus, seafan), long linear vessels or an ill-defined shape. We studied the branching pattern (dense or loose). We looked for anastomoses and loops and we determined the vessel termination (peripheral anastomotic arcade or dead-tree aspect). The presence or not of a dark perilesional halo was also noted as well as the visibility of the feeder vessel. We then used some of these characteristics to define the "pattern" of the lesion as established by Coscas et al. [10]: We considered "*pattern I*" any lesion presenting at least three of the following five characteristics (well-defined shape, dense branching pattern, presence of anastomoses and loops, peripheral anastomotic arcade and presence of a perilesional hypo-dense halo). We considered "*pattern II*" any lesion presenting at least three of the following five characteristics (ill-defined shape, loose branching pattern, absence of anastomoses and loops, dead tree-like aspect and absence of hypo-dense perilesional halo). Sensitivity of the OCT-A biomarkers of activity was determined by calculating the percentage of active lesions on MI that responded to "Pattern I". The specificity of these criteria was determined by calculating the percentage of "Pattern I" lesions that were active on MI. A lesion was considered active on MI in the presence of diffusion on FA and/or exsudative signs on structural B-scan OCT.

2.3.2. Quantitative analysis

Quantitative analyses of the MNV consisted in a semi-automated measurement its area in square millimeters, when the lesion borders were clearly defined the en face OCT-A images.

3. Results

Seventy macular neovascular lesions in 70 eyes from 55 patients were included in this study. The mean age was 70,24 years (range: 53–91). 28 were men (50,9%) and 27 were women (49,1%) with a sex ratio of 1,03. 4 eyes (5,7%) were asymptomatic. The main complaint was a decreased central vision noted in 61 eyes (87,1%). Metamorphopsia was reported in 25 eyes (35,7%). A central scotoma was reported in 20 eyes (28,6%). Eighteen eyes (25,7%) were treated with intravitreal anti-VEGF injections. The mean number of intravitreal anti-VEGF injections received was 3,5 (range: 1–8). Fifty-two eyes (74,3%) were treatment naive. The mean BCVA was 0,15 (range: 0,005–0,9). Table 1 summarizes the proportion each type of neovascular complex and the corresponding mean BCVA.

Thirty-nine lesions were active (55,7%) and thirty-one were inactive (44,3%). Sensitivity of detection of the MNV using OCT-A was 90% (63/70). Sensitivity of detection according to the type of MNV is illustrated in Table 2.

Of the 39 active lesions, 33 were detected by OCT-A (sensitivity: 84,6%). Of the 31 inactive lesions, 30 were detected by OCT-A (sensitivity: 96,8%). Of the 63 detected lesions, 26 had a well-defined shape (41,2%): 13 had the medusa shape (20,6%), 9 had the glomerulus shape

Table 1
Distribution of the different types of macular neovascularization.

Type of MNV	Number	Percentage	Mean BCVA
Type 1 MNV	40	57,1%	0,2
Type 2 MNV	15	21,4%	0,15
Mixed type 1 and type 2 MNV	1	1,4%	0,1
Type 3 MNV	1	1,4%	0,1
Retinal-choroidal anastomosis	0	0%	–
Unclassified fibrotic MNV	13	18,6%	0,02
Total	70	100%	0,15

Table 2
Sensitivity of detection of the MNV using OCT-A according to the type of MNV.

Type of MNV	Detected MNV	Undetected MNV	Total	Sensitivity of detection
Type1 MNV	34	6	40	85%
Type2 MNV	15	0	15	100%
Mixed MNV	1	0	1	100%
Type3 MNV	1	0	1	100%
Unclassified fibrotic MNV	12	1	13	92%
Total	63	7	70	90%

(14,3%) and 4 had the seafan shape (6,3%). 15 had the long linear vessels shape (23,8%) and 22 had indistinct shapes (34,9%). Fig. 1 illustrates the different MNV shapes on the en face OCT-A images. Of the 33 active MNV lesions detected on OCT-A, 23 had a well-defined shape (69,7%), 8 had an ill-defined shape (24,2%) and 2 lesions presented as long linear vessels (6,1%). Of the 30 inactive lesions detected of OCT-A, 3 had a well-defined shape, (10%), 14 had an ill-defined shape (46,7%) and 13 presented as long linear vessels (43,3%). Of the 63 detected lesions, 27 showed branching with dense vessels and numerous vascular anastomoses and loops (42,8%), 25 showed a loose branching pattern and poor anastomoses (39,7%) and 11 showed an indistinct branching pattern (17,5%).

Twenty-two lesions (34,9%) showed peripheral anastomotic arcades at the vessel termination, termination showed a dead tree aspect in 22 other lesions (34,9%) and 19 lesions showed an ill-defined termination (30,2%). Twenty-one of the 63 detected lesions showed a perilesional hypo-dense halo (33,3%).

To sum up, 26 of the 63 detected lesions were "Pattern I" (41,3%) and 37 were "pattern II" (58,7%). Of the 33 active lesions on MI detected on OCT-A, 28 were "pattern I" with a correlation rate of 84,8% between the lesion activity on MI and « pattern I » on OCT-A en face images. Considering the type of MNV, 14/21 type 1 active MNV showed "pattern I" (66,6%). 9/10 type 2 active NVM showed « pattern I » on OCT-A en face images (90%). Sensibility of OCT-A for determining the lesion activity seems higher for type 2 MNV. Of the 26 « pattern I » lesions, 25 were active on MI with a specificity of 96,1%. Of the 30 inactive lesions on MI detected on OCT-A, 29 were « pattern II » with a correlation rate of 96,6% between absence of activity signs on MI and « pattern II » on OCT-A. Of the 37 lesions showing « pattern II » on OCT-A, 29 were inactive on MI with a specificity of 78,3%.

A prominent feeder vessel was detected in 15/63 lesions (23,8%): 8/33 active lesions (24,2%) and 7/30 inactive lesions (23,3%). It was possible to calculate the lesion area for 42/63 lesions (66,7%). The mean lesion area was 3,28 mm^2 (range: 0,16–15,18 mm^2). For the 21 remaining lesions, a clear identification of the neovascular complex's borders was not possible on OCT-A en face images. The mean area of active lesions was 2,92 mm^2 (range: 0,32–11,38 mm^2). The mean area of inactive lesions was 3,86 mm^2 (range: 0,16 mm^2-15,18 mm^2).

Table 3
Distribution of the different subtypes of type 1 MNV.

Type 1 MNV	Number (n)	Percentage (%)
Active MNV	26	65%
Inactive treated MNV	4	10%
Quiescent naive MNV	10	25%
Total	40	100%
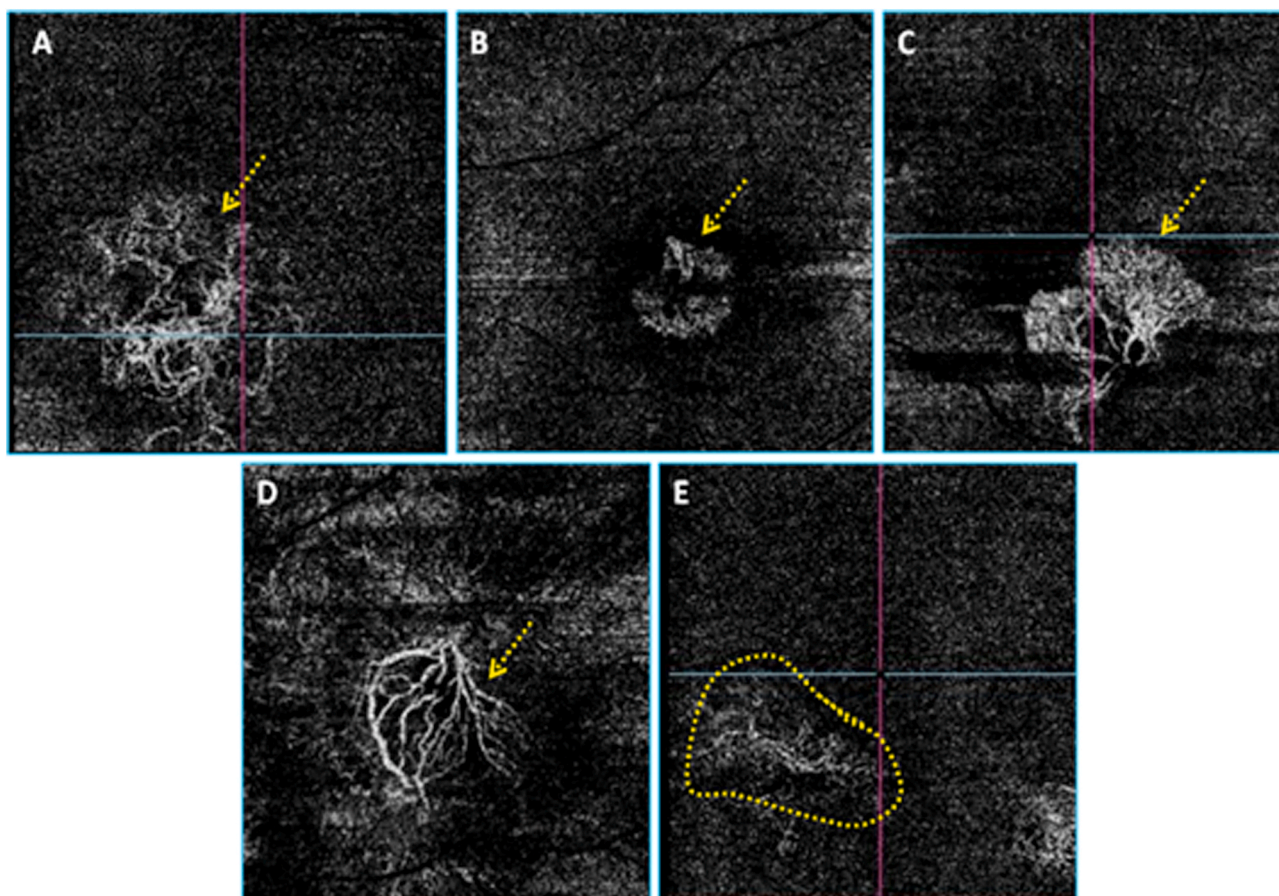
Fig. 1. Different neovascular complexes' shapes on the en face OCT-Angiograms. A: Medusa, B: Glomerulus, C: Seafan, D: Long linear vessels, E: Indistinct.

3.1. Type 1 MNV

We identified type 1 MNV in 40/72 eyes (57,1%). Table 3 summarizes the different subtypes.

The mean BCVA was 0,2 (range: 0,005–0,9). 34/40 lesions showed an evident signal on OCT-A corresponding to a sensitivity of detection of 85% all types combined. Sensitivity of detection using OCT-A was 80,7% (21/26) for active type 1 MNV, 100% (4/4) for inactive treated type 1 MNV and 90% (9/10) for quiescent naïve type1 MNV.
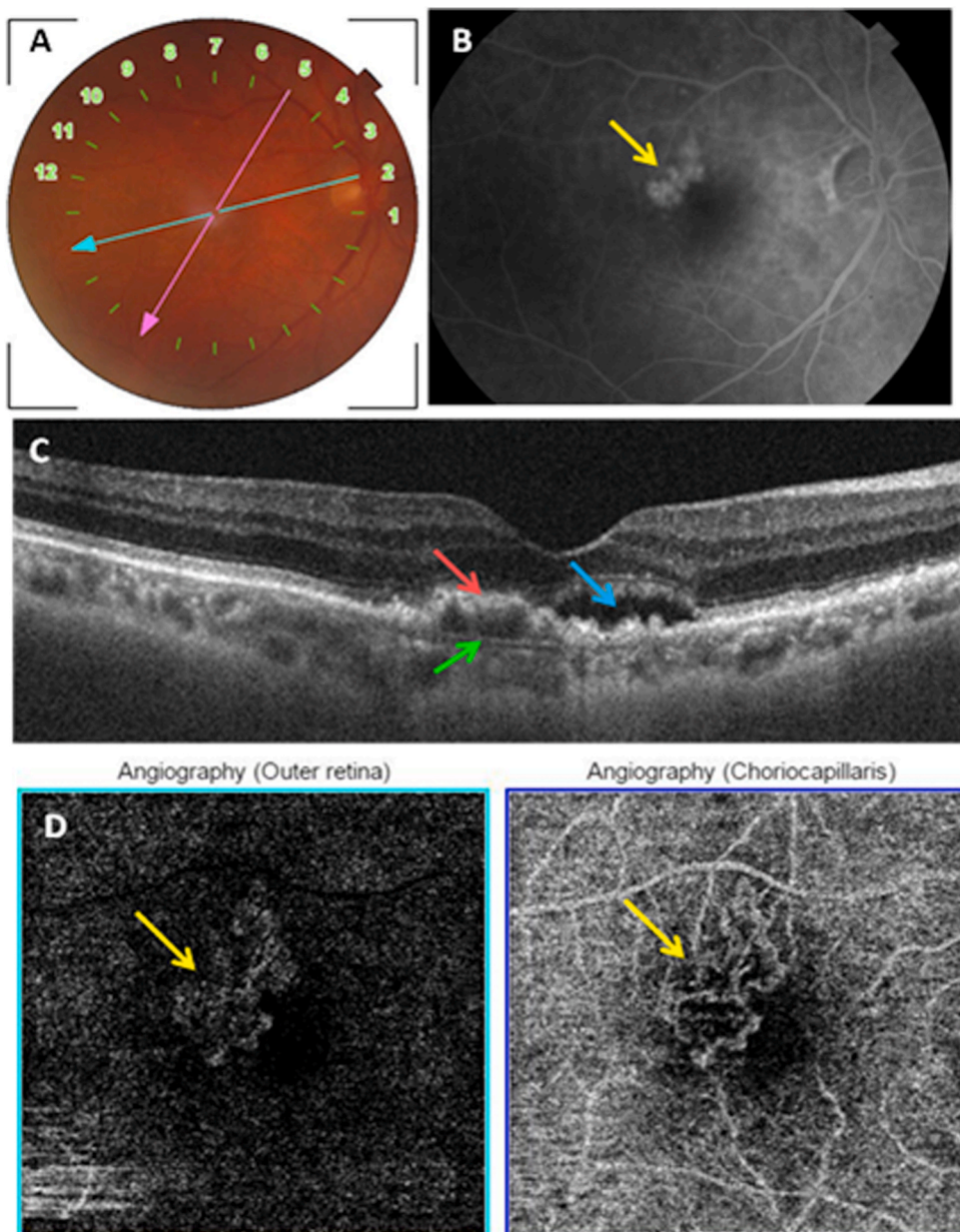
3.1.1. Active type 1 MNV

Twenty-six eyes had active type 1 MNV (37,1% of eyes with wet AMD and 65% of eyes with type 1 MNV). Mean BCVA was 0,2 (range: 0,005–0,9). 21 eyes were treatment naive (80,7%). 5 eyes received between 1 and 6 intra-vitreal anti-VEGF injections (mean: 3 injections). The neovascular complex was detected on OCT-A in 21 eyes (80,7%) (Fig. 2). The lesion showed a well-defined shape in 12/21 eyes (57,1%): a medusa-like shape in 6 eyes (28,5%), a glomerulus-like shape in 3 eyes (14,2%) and a seafan shape in 3 eyes (14,2%). One lesion had the long linear vessels shape (4,7%%). 8 lesions had an indistinct shape (38%). 14 lesions had a dense branching pattern with numerous anastomoses 66,6%), 3 lesions had a loose branching pattern and few anastomoses (14,2%) and 4 lesions had an indistinct branching pattern (19%). 12 lesions showed an anastomotic peripheral arcade termination (57,1%), 3 lesions showed a dead tree aspect termination (14,2%) and 6 lesions had an indistinct termination (28,5%). The feeder vessel was detected in 6 lesions (28,5%). A perilesional hypo-reflective halo was visible around 11 lesions (52,3%). The mean lesion area was 3,34 mm^2 (range: 0,65–11,38 mm^2) and was possible to calculate only for 14 lesions (66,7%).

3.1.2. Inactive treated type 1 MNV

4 eyes had inactive treated MNV (10% of type 1 MNV). Mean BCVA was 0,1 (range: 0,005–0,2). The mean number of intravitreal anti-VEGF injections received was 3 (range: 1–6). All 4 lesions were detected on OCT-A and showed a long linear vessels shape (100%) (Fig. 3). All had a loose branching pattern, few anastomoses and a dead tree like termination (100%). The feeder vessel was visible in one eye (25%). No lesion

Fig. 2. Multimodal imaging of an active type 1 MNV. A: Color fundus photography showing posterior pole drusen. B: Late phase of FA showing hyperfluorescent macular lesion (yellow arrow) corresponding to the MNV. C: Structural cross-sectional macular OCT (section 2) showing a hyper-reflective elevation of the RPE (red arrow) with an abnormal visualization of Bruch's membrane (green arrow) and subretinal fluid (blue arrow). D: En face OCT-A segments of the outer retina and the choriocapillaris showing a hyperflow medusa-shaped lesion. (For interpretation of the references to colour in this figure legend, the reader is referred to the Web version of this article.)
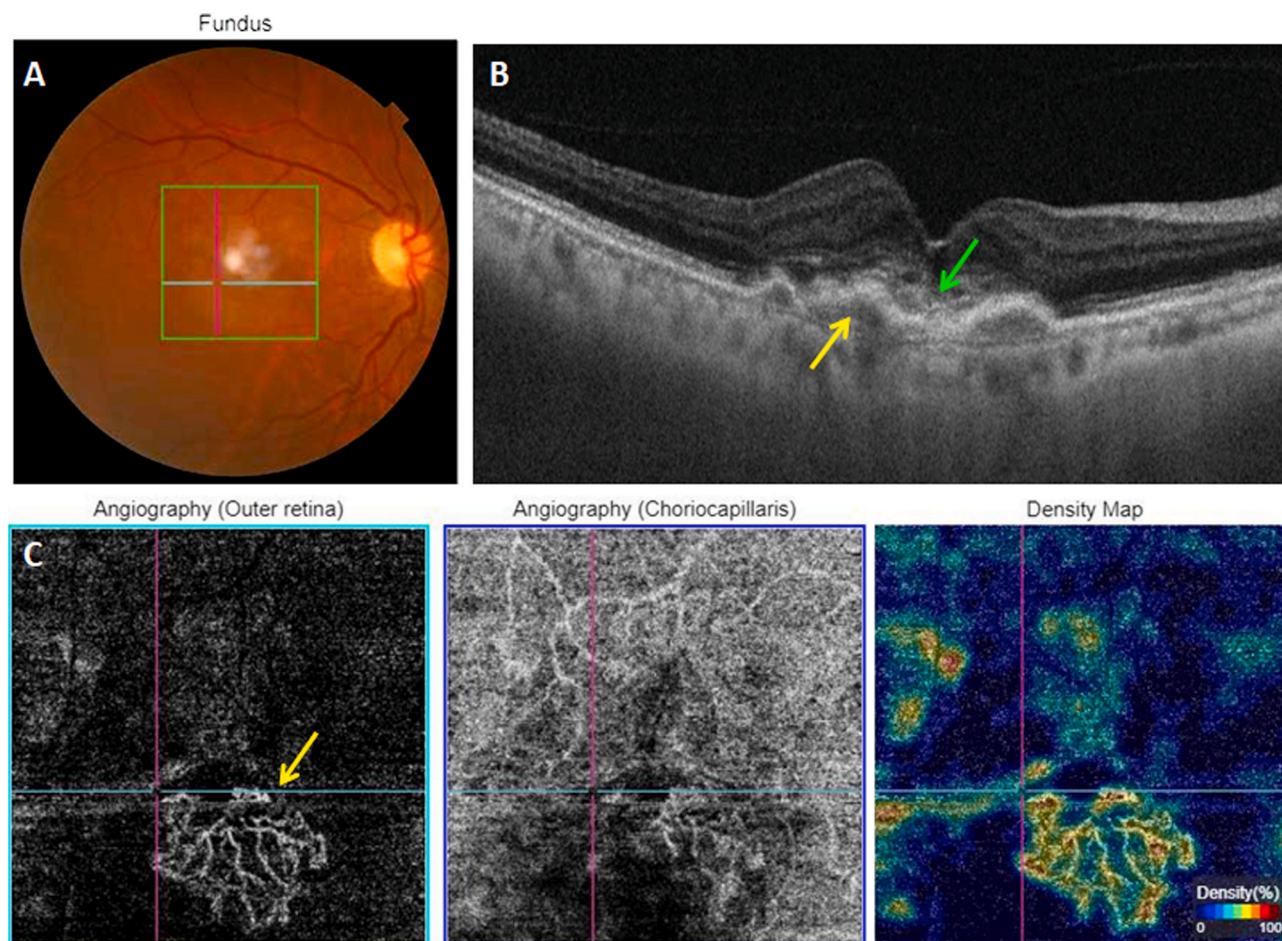
Fig. 3. Multimodal imaging of an inactive treated type 1 MNV. A: Color fundus photography. B: Structural cross-sectional macular OCT showing a hyper-reflective elevation of the RPE (yellow arrow) without exudative signs. Disorganized outer retinal layers (green arrow). C: En face OCT-A segments of the outer retina and the choriocapillaris and the corresponding density map showing a hyperflow neovascular complex. (For interpretation of the references to colour in this figure legend, the reader is referred to the Web version of this article.)

was surrounded by a hypo-reflective halo. We were able to calculate the area of 2 lesions: the first had a $1,82 \, mm^2$ area and the second $1,97 \, mm^2$.

3.1.3. Quiescent naive type 1 MNV

10 eyes had quiescent treatment-naive type 1 MNV (14,2% of eyes with wet AMD and 25% of eyes with type 1 MNV). BCVA was 0,2 (range: 0,02–0,6). OCT-A was able to detect 9 lesions (90%) (Fig. 4). 3/9 lesions showed a well-defined shape (33,3%) (medusa, glomerulus and seafan). One lesion presented as long linear vessels (11,1%) and 5 lesions showed an indistinct shape (55,5%). 5 showed a loose branching pattern and few anastomoses (55,5%). 2 lesions showed a dense branching pattern and numerous anastomoses (22,2%). 2 lesions had an indistinct branching pattern (22,2%). Vessel termination were indistinct in 4 lesions (44,4%). 4 showed a dead tree like termination (44,4%). Only one lesion showed a peripheral anastomotic arcade (11,1%). Feeder vessel was detected in 2/9 lesions (22,2%). Only one lesion was surrounded by a hypo-reflective halo (11,1%). We were able to calculate the lesion area in 7 eyes. The mean lesion area was $2,96 \, mm^2$ (range: $1,45–8,32 \, mm^2$).

3.2. Type 2 MNV

We identified type 2 MNV in 15/70 eyes (21,4%). Table 4 summarizes the distribution of the different subtypes.

The mean BCVA was 0,15 (range: 0,01–0,8). All lesions were detected on OCT-A (100%).

3.2.1. Active type 2 MNV

10 eyes had active type 2 MNV (14,2% of the eyes with wet AMD and 66,7% of the eyes with type 2 MNV). Mean BCVA was 0,10 (range: 0,02–0,4). 7 eyes were treatment-naive (70%). 3 eyes received between 3 and 8 intravitreal anti-VEGF injections (mean: 4,6 injections). All 10 lesions were detected on OCT-A (100%). Partial masking of the lesion's signal by drusen was noted in one eye (Fig. 5). The lesion's shape was well-defined in 9 eyes (90%): 4 had a medusa-like shape (40%) and 5 had a glomerulus shape (50%). One lesion presented as long linear vessels (10%). The branching pattern was dense in 9 lesions (90%). Only one lesion had a loose branching pattern and few anastomoses (10%). 7 lesions had a peripheral anastomotic arcade termination (70%). One lesion had a dead tree like termination and 2 lesions showed indistinct termination. The feeder vessel was detected in 2 lesions (20%). A hypo-reflective perilesional halo surrounded 8 lesions (80%). We were able to calculate the area of all 10 lesions. The mean lesion area was $2,21 \, mm^2$ (range: $0,32–7,59 \, mm^2$).

3.2.2. Inactive type 2 MNV

5 eyes had inactive type 2 MNV (7,1% of the eyes with wet AMD and 33,3% of the eyes with type 2 MNV). BCVA was 0,24 (range: 0,01–0,8). All eyes were treatment-naive. All 5 lesions were detected on OCT-A (100%) (Fig. 6). 2 lesions showed an ill-defined shape (40%). 3 lesions presented as long linear vessels (60%). No lesion had a well-defined shape. All 5 lesions showed a loose branching pattern and few anastomoses (100%). 4 had a dead tree like termination (80%) and one lesion
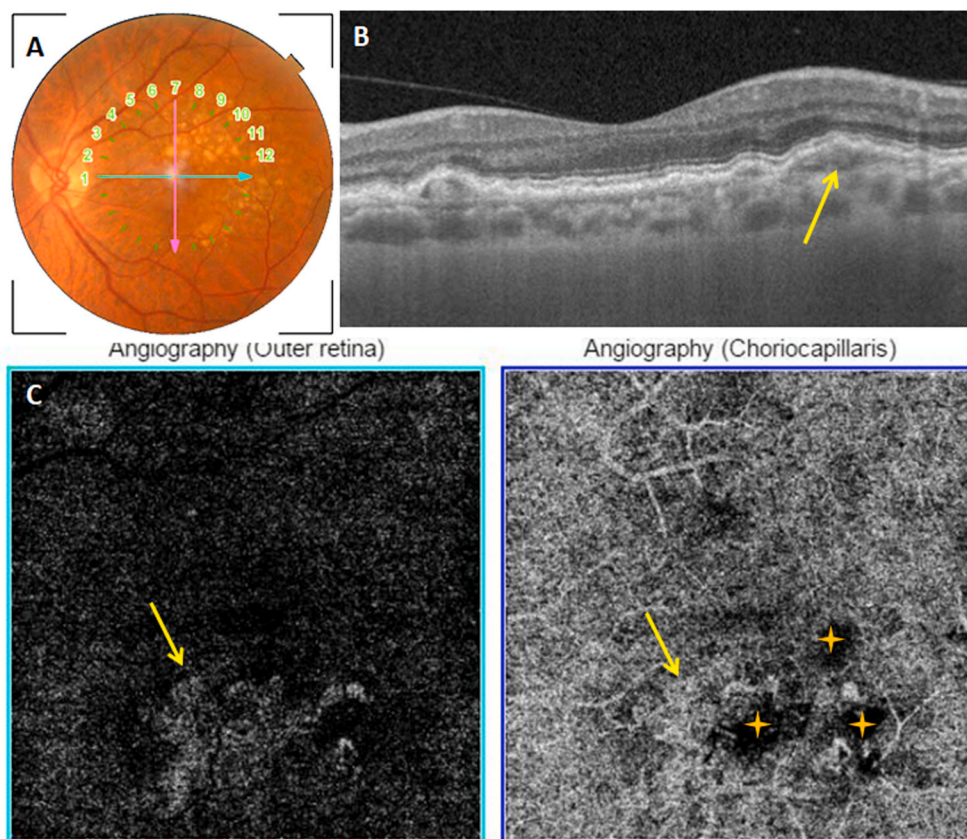
Fig. 4. Quiescent naive type 1 MNV. A: Color fundus photography showing posterior pole drusen. B: Structural cross-sectional macular OCT (section 7) showing a hyper-reflective elevation of the RPE (yellow arrow) C: En face OCT-A segments of the outer retina and the choriocapillaris showing a hyperflow medusa-shaped lesion (yellow arrow). Drusen's masking effect (yellow stars). (For interpretation of the references to colour in this figure legend, the reader is referred to the Web version of this article.)

Table 4
Distribution of the different subtypes of type 2 MNV.

Type 2 MNV	Number (n)	Percentage (%)
Active type 2 MNV	10	66,7
Inactive type 2 MNV	5	33,3
Total	15	100

had an ill-defined termination (20%). The feeder vessel was detected in 2 lesions (40%).

No lesion was surrounded by a hypo-reflective halo. We were able to calculate the lesion's area in 3 eyes. The mean area was 2,65 mm^2 (range: 0,65–3,87 mm^2).

3.3. Mixed type 1 and type 2 MNV

We identified a mixed type 1 and type 2 MNV in one eye (1,4%). The lesion consisted of an active type 1 component and an inactive type 2 component. BCVA in this eye was 0,1. Previous treatment with 3 intravitreal anti-VEGF injections had been reported. The lesion showed a clear signal on OCT-A. Signal masking by hard exudates was noted, clearer on the choriocapillaris slab (Fig. 7). The first component had a medusa-like shape, a dense branching pattern with numerous anastomoses, an peripheral anastomotic arcade. The second component presented as long linear vessels, had a loose branching pattern with few anastomoses and a dead tree like termination. We could not identify any feeder vessel, and the lesion was not surrounded by a perilesional hypo-reflective halo. The lesion's area was 5,13 mm^2 corresponding to the sum of the areas of its 2 components.

3.4. Type 3 MNV

We identified a type 3 MNV in one eye (1,4%). BCVA was 0,1. The

lesion was treatment-naïve. It presented an clear signal on OCT-A (Fig. 8). Shape, branching pattern and vessel termination were indistinct. The feeder vessel was not detected. We could not identify any perilesional hyporéflective halo. The lesion had a relatively small area of 0,16 mm^2.

### 3.5. Retinal choroidal anastomosis (RCA)

We could not identify any RCA.

3.6. Unclassified fibrotic MNV

13 eyes had unclassified fibrotic MNV (18,5%). The mean BCVA was 0,02 (range: 0,005–0,05). 8 eyes were treatment-naive (61,5%). 5 eyes received a mean of 4 intravitreal anti-VEGF injections (range: 3–6 injections). The lesion showed an evident signal on OCT-A in 12 eyes (92,3%) (Fig. 9). The lesion's shape was ill-defined in 6 eyes (50%). 5 presented as long linear vessels (41,6%). Only one lesion had a well-defined shape (medusa-like) (8,3%). The branching pattern was ill-defined in 5 lesions (41,6%). 6 lesions showed a loose branching pattern (50%). Only one lesion showed a dense branching pattern and numerous vascular anastomoses (8,3%). The lesion's termination was ill-defined in 5 eyes (41,6%). 6 lesions showed a dead tree like termination (50%). Only one lesion showed a peripheral anastomotic arcade (8,3%). The feeder vessel was detected in 2 lesions (16,6%). A perilesional dark halo was detected around one lesion (8,3%). It was possible to calculate the lesion's are in only 4 eyes. The mean calculated area was 7,81 mm^2 (range: 2,03–15,18 mm^2).

4. Discussion

Wet AMD is characterized by the invasion of the macular region by a neovascular proliferation [11]. The diagnosis, classification and
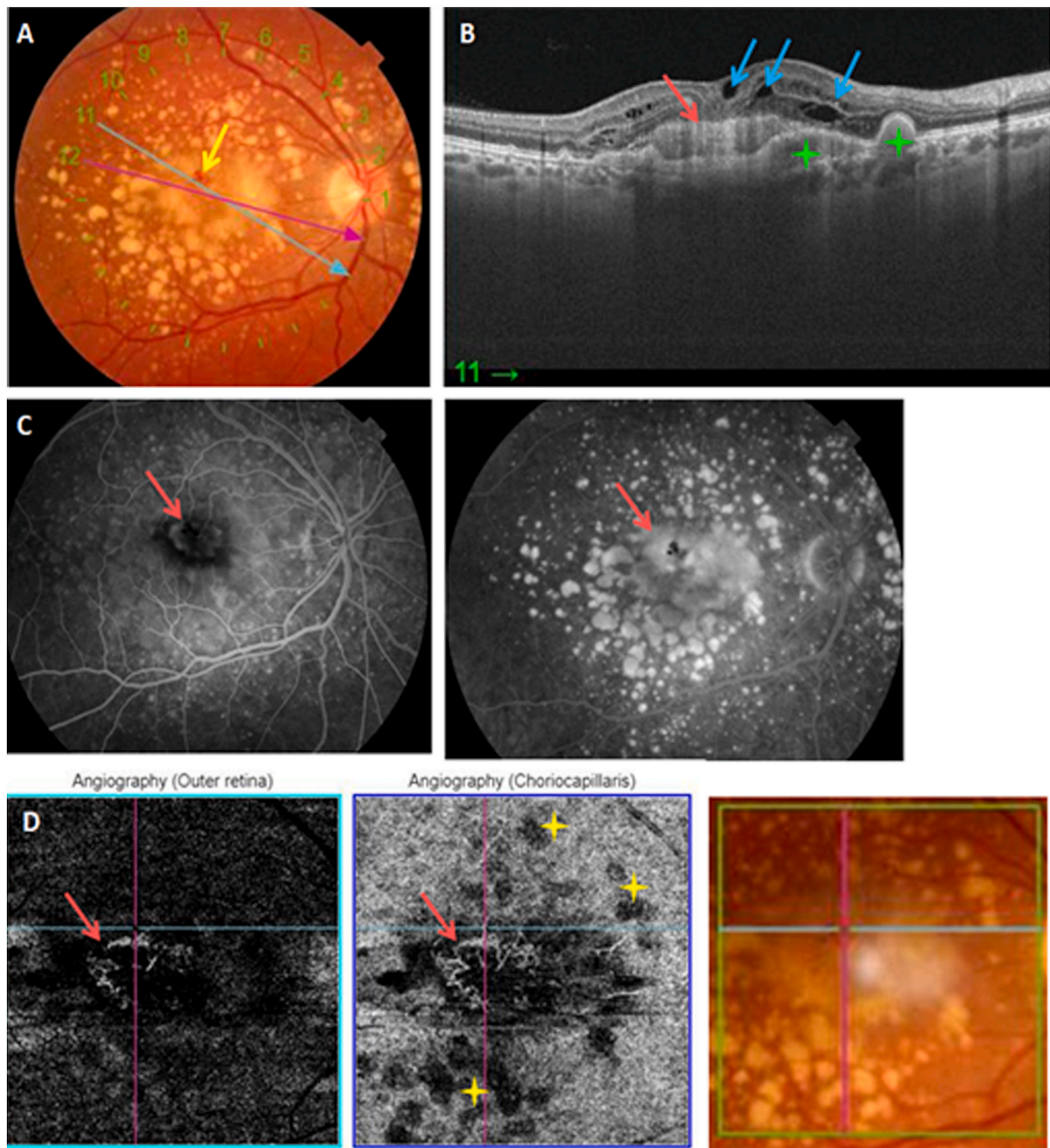
Fig. 5. Multimodal imaging of an active type 2 MNV. **A:** Color fundus photography showing posterior pole drusen and a yellow-grey macular lesion with an adjacent hemorrhage (yellow arrow). **B:** Structural cross-sectional macular OCT (section 11) showing drusenoid pigment epithelial detachments (green stars), intra-retinal fluid (blue arrows) and a hyperreflective preretinal lesion (yellow arrow). **C:** Early and late phase of FA showing an initially hypofluorescent lesion that drowns in the drusen's hyperfluorescence in the late phase (red arrow. **D:** En face OCT-A segments of the outer retina and the choriocapillaris showing a hyperflow medusa-shaped lesion. Partial masking by drusen (yellow stars). (For interpretation of the references to colour in this figure legend, the reader is referred to the Web version of this article.)

monitoring of this pathology were mainly based on retinal FA, long considered as the gold standard [12]. Since its introduction, OCT-A is gaining in popularity in the diagnosis and management of wet AMD since it offers high-resolution images without any need for dye injections, compared with traditional angiography.

4.1. Detection of MNV

Several authors have been interested in the sensitivity and specificity of OCT-A for the diagnosis of MNV in AMD. The results vary across studies and seem to be influenced by the equipment used as well as the

MNV type. Results are summarized in Tables 5 and 6.

4.2. Assessment of exudative activity

Before the advent of OCT-A, the assessment of the MNV's exudative activity was based on the presence of leakages on FA and exsudative signs on structural OCT. Coscas et al. [10] first defined qualitative bio-markers of exudative activity based on the morphology of the MNV on the OCT-Angiograms in eyes undergoing anti-angiogenic treatment: a small vascular caliber, a peripheral anastomotic arcade and the presence of a perilesional halo sign were particularly associated with the
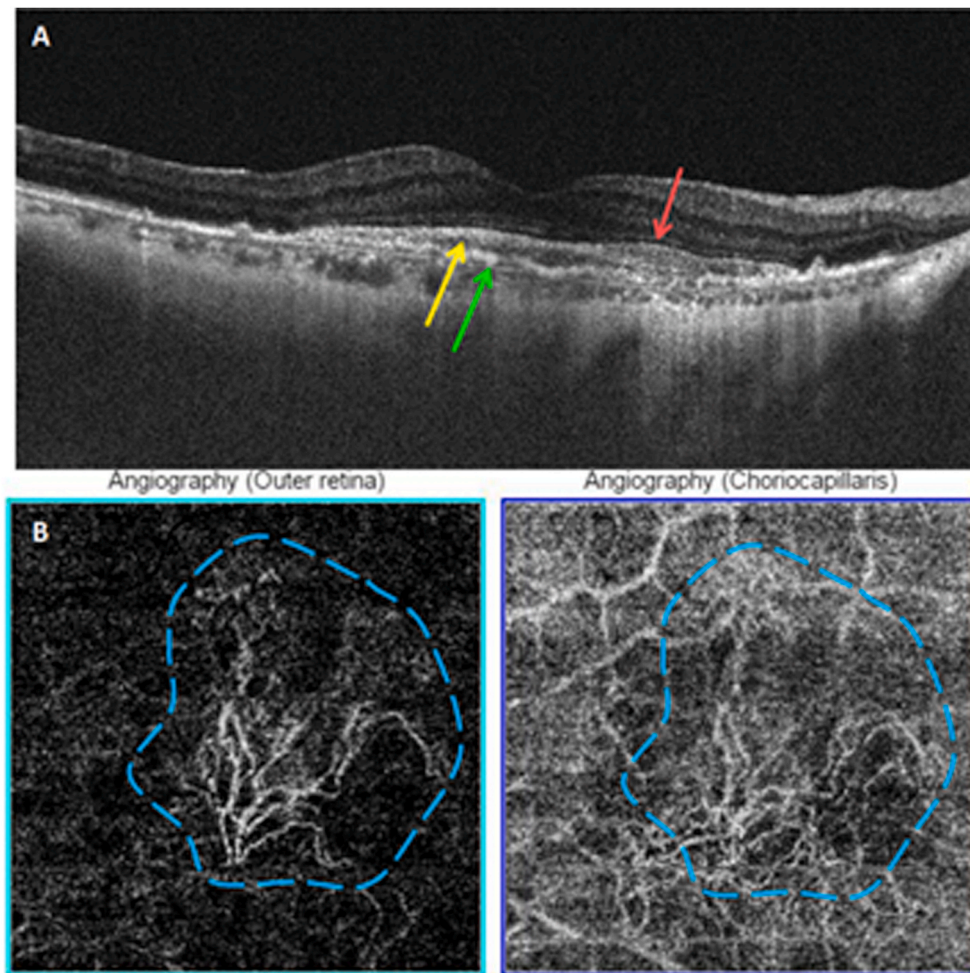
Fig. 6. Inactive type 2 MNV. A: Structural cross-sectional macular showing a hyperreflective preretinal lesion (yellows arrow), irregular RPE (green arrow) and preserved outer retinal layer (red arrow). B: En face OCT-A segments of the outer retina and the choriocapillaris showing hyperflow long linear vessels. (For interpretation of the references to colour in this figure legend, the reader is referred to the Web version of this article.)

exudative activity of the MNV lesion. Authors reported a 94.9% correspondence between "Pattern I" on OCT-A and lesions's activity on MI, and of 90.5% between "Pattern II" on OCT-A and the absence of activity signs on MI.

In addition to these qualitative criteria, a quantitative analysis of the MNV lesion is also possible using OCT-A in order de assess to lesions's. In this context, numerous authors have studied the evolution of certain quantitative parameters characterizing these lesions under anti-VEGF treatment. Coscas et al. [16] demonstrated in a study published in 2018 that quantification of the blood flow area combined with morphological parameters made it possible to distinguish active MNV from inactive MNV "in remission". Von Der Emde al. [17] published a study in 2020 that evaluated the qualitative criteria proposed by Coascas et al. [10] as well as additional quantitative of exudative activity: vessel length, vessel density and branching index. In our study, we adopted the qualitative activity criteria proposed by Coscas et al. [10]. Each criterion will be detailed in a separate chapter. No quantitative criteria have been adopted for lack of software.

4.2.1. Shape

Karacorlu et al. [18] compared the different shapes observed on OCT-Angiograms of MNV lesions in naive eyes, eyes undergoing anti-angiogenic treatment and eyes having completed treatment, in a recently published retrospective study enrolling 184 eye. The lesion's type and clinical activity were determined on fundoscopy and structural OCT. A well defined shape was noted in 69% of treatment-naïve eyes

and 77% of eyes undergoing treatment. Long linear vessels were noted in 53% of eyes having completed treatment. All active lesions had either a well-defined shape (medusa or seafan) or an ill-defined shape. No active lesions presented as long linear vessels. In our study, a well defined shape was noted in 41,2% eyes, an ill-defined shape in 34,9% and long linear vessels were noted in 23,8% eyes. 69,7% of active lesions had a well-defined, 24,2% had an ill-defined shape and 6,1% presented as long linear vessels. 88,5% of lesions having a well-defined shape were active 88,5% with a good specificity of this criteria. 10% of inactive lesions had an well-defined shape, 46,7% had an ill-defined shape and 43,3% presented as long linear vessels. 63,6% of lesions with an ill-defined shape were inactive and 36,3% were active.

Parmi les 22 lésions de forme mal définie, 14 étaient inactives (63,6%) et 8 étaient actives (36,3%). The ill-defined shape does not seem to be a good criterion for assessing the inactivity of the lesion.

4.2.1.1. Type 1 MNV

Several studies have described the different possible morphologies of type 1 MNV on OCT-A. Many terms have been used: "umbrella", "medusa", "seafan", "tangled vascular network", "pruned tree" and "flowering tree" [19–21]. Kuehlewein et al. [22] reported that type 1 MNV took two distinct shape on OCT-A: The "medusa" shape characterized by vascular ramifications from the center of the lesion in all directions and the "fan" shape characterized by vascular ramifications in a single direction on one side of the lesion. The authors did not note any statistically significant correlations between the shape and the number
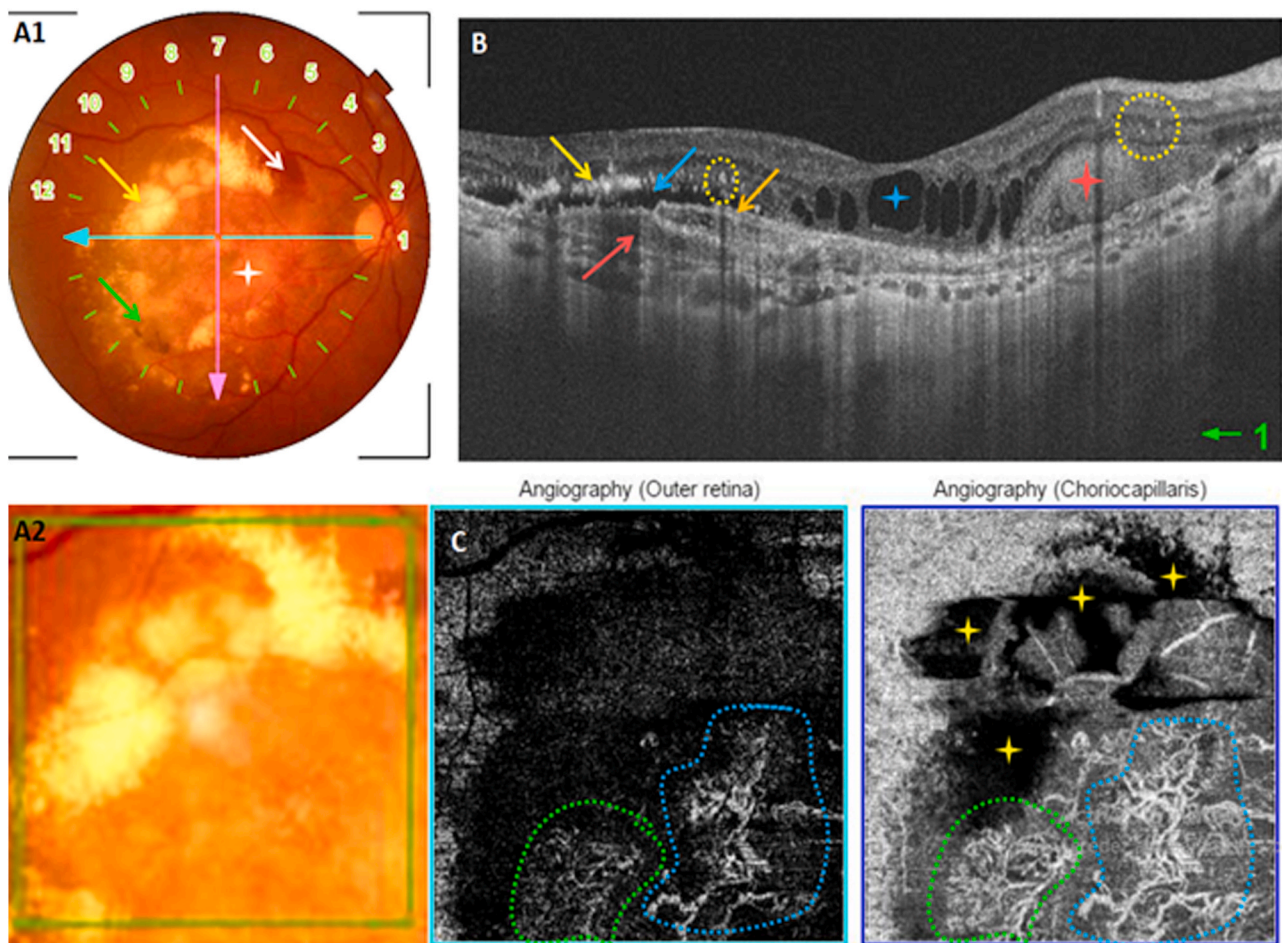
Fig. 7. Mixed type 1 and type 2 MNV. A: Color fundus photography showing a macular yellowish lesion (white star), RPE alterations (green arrow), hard exudates (yellow arrow) and a macular hemorrhage (white arrow). B: Structural cross-sectional macular OCT (section 1) showing two hyperreflective lesions on either side of the RPE (red and orange arrows), subretinal fluid (blue arrow), intra-retinal exudates (yellow arrow), intra-retinal fluid (blue star), subretinal hyperreflective material (red star) and intra-retinal hyperreflective dots (yellow circle). C: En face OCT-A segments of the outer retina and the choriocapillaris showing two hyperflow lesions (blue and green). Important masking by exudates (yellow stars). (For interpretation of the references to colour in this figure legend, the reader is referred to the Web version of this article.)

of intravitreal anti-VEGF injections received. Carnevali et al. [23] described two shapes of quiescent lesions detected in OCT-A: the "circular" shape noted in 44.44% of the eyes and the "irregular" shape noted in 55.56% of the eyes. In our study, 100% of type 1 inactive MNV lesions presented as long linear vessels. 33,3% of eyes with quiescent naive MNV had a well-defined shape, 55,5% had an ill-defined shape and 11, 1% presented as long linear vessels.

4.2.1.2. Type 2 MNV

Type 2 MNV takes characteristic shapes on en face OCT-A [24]. The neovascular membrane appears either "medusa" or "glomerulus" shaped on the external retina (ER) slab [25]. The "medusa" shape is characterized by a roughly oval image made up of a dense, high-flow capillary network. The "glomerulus" shape is generally rounded, well defined, rich in fine and dense capillaries. In our study, 90% of type 2 active MNV had a well-defined shape (40% "medusa" shape and 50% "glomerulus" shape). 10% presented as long linear vessels. 40% of type 2 inactive MNV had an ill-defined shape and 60% presented as long linear vessels. No type 2 inactive MNV showed a well-defined shape.

4.2.1.3. Type 3 MNV

The "tuft-shaped" appearance is a widely used term in the literature to refer to the most common shape of type 3 MNV on en face OCT-Angiograms [26], observed mainly on the ER slab. This tufted shape

corresponds on the choriocapillaris slab to a "clew-like" appearance also described by certain authors [26]. Kuehlewein et al. [19] described the type 3 MNV on the en face OCT-Angiogram as a small "shiny" hyperdense tuft made of small, high-flow curvilinear vessels. The smaller the lesion's size, the more difficult it was to distinguish its vascular and we could only visualize a bright round or ellipsoid neovascular complex. It was possible to identify small caliber curvilinear vessels in the larger lesions.

In our study, our only type 3 MNV lesion presented on the en face OCT-Angiograms as a strongly hyper-dense image on the DCP slab with an ill-defined shape resembling of the "tufted" appearance.

4.2.1.4. Unclassified fibrotic MNV

Miere et al. [27] reported three possible shape of the macular neovascular complex detected on OCT-A in eyes with subretinal fibrosis secondary to AMD: "pruned vascular tree" (53.1%), "tangled capillary network" (28, 6%) and "vascular loop" (51.0%). In our study, 50% of the unclassified fibrotic MNV had an ill-defined shape, 41.6% presented as long linear vessels) and 8,3% had a well-defined shape ("medusa" shape).

4.2.2. Branching pattern, anastomoses and vessel's termination

Al-Sheikh et al. [28] described the different qualitative and quantitative biomarkers of exudative activity of MNV on OCT-A in a study
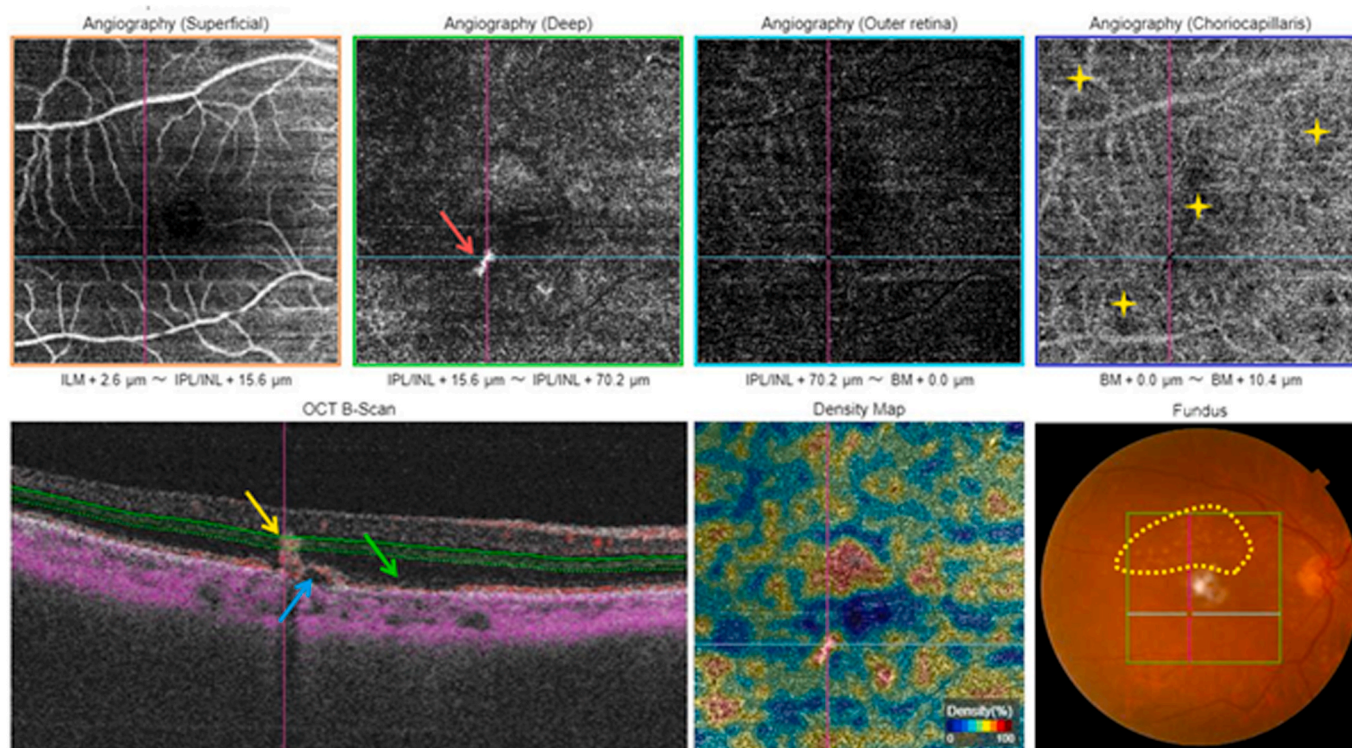
Fig. 8. Macular OCT-A report of a type 3 MNV showing an ill-defined small hyperflow lesion on the deep capillary plexus slab (red arrow). Note the intra-lesional flow in red on the cross-sectional OCT-Angiogram (yellow arrow). Serous PED (blue arrow). Localized alteration of the outer retinal layers (green arrow). Drusen in the posterior pole (yellow circle). (For interpretation of the references to colour in this figure legend, the reader is referred to the Web version of this article.)

enrolling 11 eyes with active MNV before and after treatment and 20 eyes with inactive MNV. A dense branching pattern made up of numerous fine capillaries was noted in 81.81% of active lesions and in 63.63% of active lesions after anti-angiogenic treatment, against 30% of inactive lesions. According to the authors, this parameter would be reliable for distinguishing active lesions from inactive lesions, but does not allow differentiating active lesions before treatment from active lesions after treatment. Peripheral anastomotic arcade was noted in 81.81% of active neovascular lesions and persisted after treatment, and in 40% of inactive lesions. This parameter was also interesting for the distinction between active and inactive lesion. It is interesting to note that on the other hand, the vascular caliber was larger for inactive lesions and the vessels seemed more dilated compared to those of active lesions.

Coscas et al. [10] had previously identified these parameters (dense branching pattern and anastomotic peripheral arcade as well as the numerous vascular loops) as biomarkers of lesions' activity on OCT-A. However, they are insufficient on their own and need to be confronted with other OCT-Angiographic markers. In their study, 75% of the lesions had a dense branching pattern made up of many fine capillaries and 25% had a loose branching pattern made up of few large vessels. Interesting finding, 89.3% of lesions with a dense branching pattern were classified as Pattern I. The lesion was rich in loops and anastomoses in 75% of eyes and 98.3% of them were classified as Pattern I.

Regarding the termination, 73.7% of the lesions had a peripheral anastomotic arcade and 26.3% had a "dead tree" termination. All lesions with anastomotic peripheral arcade were ultimately classified Pattern I. Sulzbacher et al. [29] reported a dense branching pattern in 12/14 naive lesions and a loose or unidentifiable branching pattern in 2/14 lesions. Regarding the treated lesions, 43.2% had a dense capillary network, 27% had a loose network, 14.9% had a mixed network and 14.9% had an unidentifiable branching pattern. In addition, clinical correlations had revealed a longer duration of disease progression for lesions with a loose network. A recent study published in 2020 by Solecki et al. [30]

investigated the predictors of exudative activity of quiescent MNV lesions using OCT-A. Among these factors, the lesion's branching pattern was analyzed and a statistically significant correlation was established between the increase in the vascular network density during follow-up and the appearance of exudative signs. In our study, 75,8% of active lesions had a dense branching pattern), 12,1% had a loose branching pattern and 12,1% had an ill-defined branching pattern. 92,6% of the lesions showing a dense branching pattern were active on MI with a good specificity of this criterion. On the other hand 63,6% of the active lesions ended with a peripheral anastomotic arcade, 12,1% ended with a "dead-tree" aspect and 24,2% had an ill-defined termination. 95,5% of the lesions with an anastomotic peripheral arcade were active on MI with a good specificity of this criterion.

70% of inactive lesions had a loose branching pattern, 23,3% had an ill-defined branching pattern and only 6,7% had a dense branching pattern. 84% of the lesions showing a loose branching pattern were inactive on MI with a good specificity of this criterion. 60% of inactive lesions ended with a « dead-tree » aspect), 36,7% had an ill-defined termination and 3,3% ended with an anastomotic peripheral arcade. 81,8% of the lesions ending with a dead-tree aspect were inactive on MI with a good specificity of this criterion.

4.2.2.1. Type 1 MNV

Spaide [31] and Muakkassa et al. [32] reported that early type 1 MNV before treatment had a dense branching pattern made of fine tangled vessels on en face OCT-A. Carnevali et al. [23] noted that 83% of eyes with quiescent naive MNV showed a well defined branching pattern and 17% showed an ill-defined branching pattern. 50% of the lesions had small vascular loops on its borders and 33,% had large anastomotic vascular loops. In our study, 66,6% of active type 1 MNV showed dense branching patterns and numerous anastomoses, 14,2% had a loose branching pattern and few anatomoses and 19% had an ill-defined branching pattern. 57,1% ended with a peripheral anastomotic arcade, 14,2% ended in a dead tree aspect and 28,5% had an ill-defined
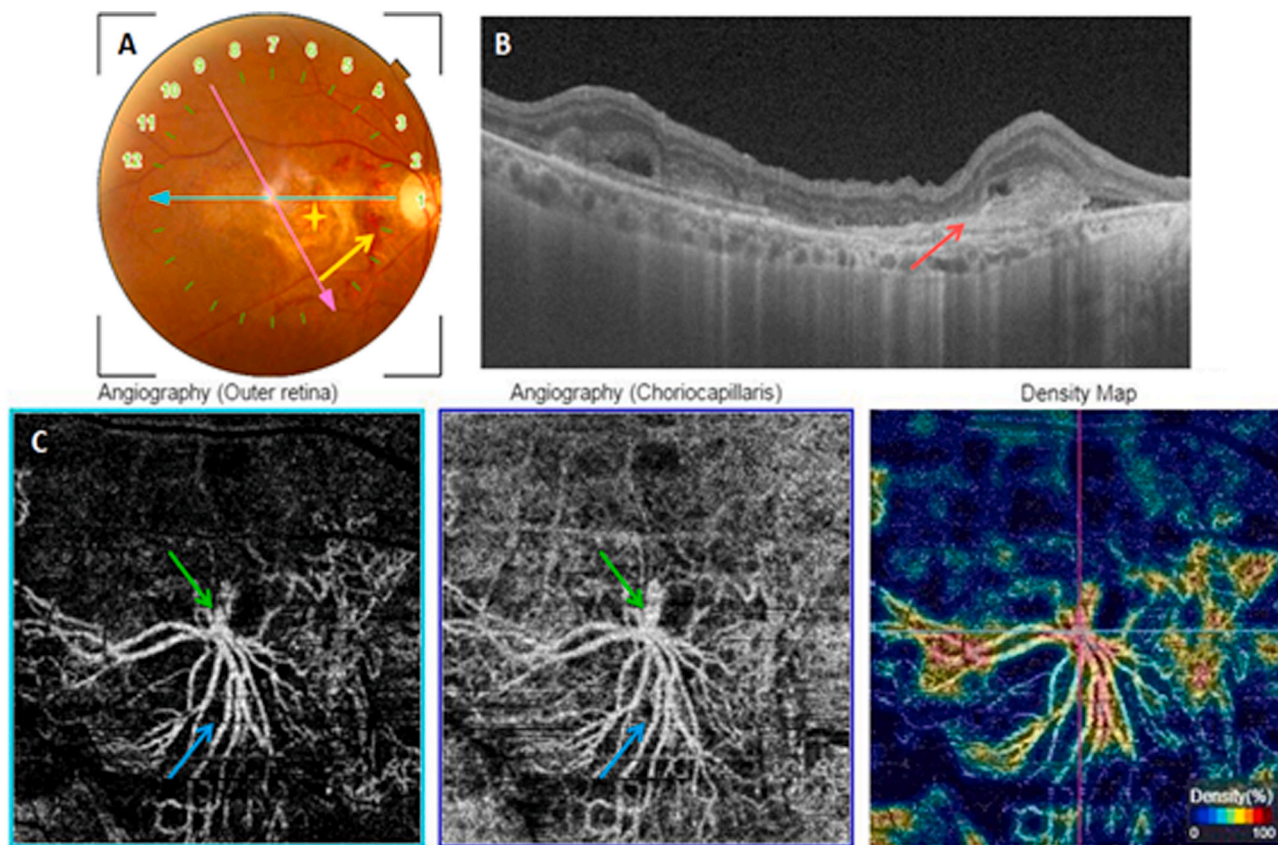
Fig. 9. Unclassified fibrotic MNV. A: Color fundus photography showing a macular fibrotic scar (yellow star) with an adjacent hemorrhage (yellow arrow). B: Structural cross-sectional macular OCT (section 1) showing a hyperreflective preretinal lesion (red arrow). C: En face OCT-A segments of the outer retina and the choriocapillaris with the corresponding density map showing hyperflow long linear vessels (blue arrow). The lesion's feeder vessel is identifiable (green arrow). (For interpretation of the references to colour in this figure legend, the reader is referred to the Web version of this article.)

Table 5
Sensitivity and specificity of OCT-A for the detection of MNV in wet AMD.

Study	Sensitivity (n)	Specificity (n)
Faridi et al. [13] (SD-OCT-A; 2017)	A = 81% (26/32) B = 100% (32/32)	A = 98% (39/40) B = 100% (40/40)
Ahmed et al. [14] SS-OCT-A; 2018)	76% (81/107)	100%(49/49)
Yeo et al. [15] (SS-OCT-A; 2019)	80,7% (42/52)	Not available
Notre étude (SS-OCT-A; 2019)	90% (63/70)	Not available

A: OCT-A en face; B: OCT-A en face and cross-sectional OCT-A.

Table 6
Sensitivity of OCT-A for the detection of MNV in wet AMD according to the lesion's type.

Study	Sensitivity of detection using OCT-A (n)				
	Type 1 MNV	Type 2 MNV	Mixed MNV	Type 3 MNV	Unclassified MNV
Yeo et al. [15] (SS-OCT-A; 2019)	73,5% (25/34)	100% (9/9)	/	88,9% (8/9)	/
Our study (SS-OCT-A; 2019)	85% (34/40)	100% (15/15)	100% (1/1)	100% (1/1)	92% (12/13)

termination. All type1 inactive treated MNV lesions had a loose branching pattern and a dead tree termination. 55,5% of type 1 quiescent naive MNV had a loose branching pattern with few anatomoses), 22,2% had a dense branching pattern with numerous anastomoses and 22,2% had an ill-defined branching pattern. 44,4% had an ill-defined

termination, 44,4% had a dead tree termination and 11,1% ended with a peripheral anastomotic arcade.

4.2.2.2. Type 2 MNV

In a review published by Souied et al. [24], the authors described a morphological change of the type 2 neovascular complex on en face OCT-Angiograms after anti-angiogenic treatment mainly affecting the lesion's branching pattern becoming less compact with decreased capillary density parallel to decreased activity on MI. In our study, 90% of active type 2 MNV had a dense branching pattern and numerous anastomoses and only 10% had a loose branching pattern and few anastomoses. 70% showed a peripheral anastomotic arcade, 10% ended with a dead tree aspect and 20% had an ill-defined termination. All active type 2 lesions had a loose branching pattern and few anastomoses. 80% ended in a dead tree aspect and 20% had an ill-defined termination.

4.2.2.3. Unclassified fibrotic MNV

Miere et al. [27] noted that all unclassified fibrotic lesions presented as rarefied networks made of large mature vessels without any vascular loops. No lesion was made of fine dense capillaries. Flow void areas were noted in 37% of the eyes. In our study, 41,6% of unclassified fibrotic lesions had an ill-defined branching pattern and 50% were poor in anastomoses. 8,3% had dense branching patterns. 41,6% had an ill-defined termination, 50% ended in a dead tree aspect and 8,3% ended in a peripheral anastomotic arcade.

4.2.3. Perilesional hypodense halo

Coscas et al. [10] noted a halo sign **around** 81% of the active lesions

and 82% of the lesions surrounded by a perilesional dark halo were classified "Pattern I". Solecki et al. [30] analyzed the predictors of exudation of quiescent neovascular complexes on OCT-A and established a statistically significant correlation between the appearance of a dark halo around the lesion and the risk of exudation. On the other hand, Coscas et al. [33] were interested in the predictive role of different qualitative OCT-Angiographic parameters in the assessment of exudative activity of MNV lesions in order to initiate antiangiogenic treatment. 71% of the lesions were active on structural OCT, but a dark perilesional halo was present in only 54.8% of cases. This criterion alone had no statistically significant correlation with the treatment indication and was associated with a relatively low risk of exudation compared to the criteria "dense branching pattern" and "peripheral arcade" which were associated with the highest relative risk of exudation. Similarly, Von Der Emde et al. [17] reported a halo sign in 66.7% of the lesions all types combined, but its prevalence was not significantly different between the 3 groups of lesions studied: active, inactive and quiescent naïve (respective values of 56.3%, 81.8% and 87.5%). In our study, we noted a halo sign around 60.6% of the detected active lesions and around a single inactive lesion (3.3%). Interestingly, 95.2% of lesions surrounded by a dark halo were inactive on MI, with an excellent specificity of this criterion. Considering the type of the lesion, a dark perilesional halo was visible around all active type 2 lesions in a study published by El Ameen et al. [25]. It was more evident on the choriocapillaris slab but was also visible on the ER slab. In our study, a dark perilesional halo was present around 80% of active type 2 lesions and around 52.3% of active type 1 lesions. The type 3 lesion was not surrounded by a dark perilesional halo. Souied et al. [24] detected a dark perilesional halo around 65% of the lesions. A statistically significant correlation was established between the presence of vascular loops and perilesional dark halo. Miere et al. [27] noted a dark perilesional halo around 70.37% of fibrotic lesions. In our study, a perilesional dark halo was present around a single unclassified fibrotic lesion (8.3%).

4.3. Feeder vessel

The detection of the MNV's feeder vessel, or feeder trunk, using OCT-A has been frequently reported in the literature. According to Souied et al. [34], one MNV lesion may have more one feeder vessel. OCT-A could also detect draining vessels but the distinction between the two is exceptionally possible. A feeder vessel connecting the MNV to the choroid was detected on OCT-Angiograms in 20% of the lesions studied by Jia et al. [35] (type 1 and type 2 combined). Considering the lesion's exudative activity, Al-Sheikh et al. [28] detected the lesion's feeder vessel using OCT-A in 63.6% of active lesions and 100% of inactive lesions. In our study, OCT-A identified the feeder vessel in 23.8% of the lesions all types combined: 24.2% of active lesions and 23.3% of inactive lesions.

4.3.1. Type 1 MNV

Kuehlewein et *al.* [22] identified a large central feeder trunk in 72% of the type 1 MNV lesions. In our study, we detected the feeder trunk in 28,5% of the active lesions and in 25% of the inactive treated lesions. The absence of a detectable feeder trunk in quiescent naive lesions would be a protective factor against exudative activity according to Carnevali et al. [23]. The authors identified the feeder trunk in 11,11% of quiescent naïve lesions. We identified the feeder trunk in 22,2% of quiescent naive lesions in our study.

4.3.2. Type 2 MNV

El Ameen et al. [25] reported that 71.43% of the type 2 lesions were connected on the OCT-Angiograms to a larger central vascular trunk which seemed to continue in depth towards the choroidal layers, corresponding to the feeder vessel. In our study, we detected a feeder vessel in 26,6% of the type 2 lesions: 20% of the active type 2 lesions and 40% of the inactive type 2 lesions.

4.3.3. Type 3 MNV

Kuehlewein et al. [19] identified a feeder vessel communicating with the deep retinal capillary plexus using OCT-A in 100% of the type 3 lesions. In our study, the type 3 lesion detected was ill-defined on OCT-A thus the feeder vessel could not be identified.

4.4. Lesion's area

The semi-automatic quantification of neovascular complex's area on the en face OCT-Angiograms relies on a manual delineation of the lesion's borders by digital tracing tools. The indirect visualization of the MNV by detecting the flow signal rather than the lesion itself could question the reliability of this measurement. Amoroso et al. [36] noted an excellent reproducibility of the lesion's area measurement on the en face OCT-Angiograms. In our study, we were able de calculate the lesion's are in 66,7% of the lesions, all types combined. For the remaining lesions, we were not able to correctly delimit the neovascular complex due to fuzzy borders and/or going beyond the acquisition cube limits, thus making semi-automatic area measurement impossible. Al-Sheikh et al. noted that the average lesion's area in inactive neovascular complexes was approximately 15% less than that of the active lesions with respective values of 3.503 mm^2 and 4.066 mm^2. In our study, the mean area of inactive lesions was slightly larger than that of active lesions with respective values of 3.86 mm^2 and 2.92 mm2 . Type 1 lesions (3.09 mm^2) had a larger area than type 2 lesions (2.31 mm^2). The only type 3 lesion studied had a very small area (0.16 mm^2). Unclassified fibrotic lesions had the largest mean area (7.81 mm^2) although manual delimitation of the lesion was not possible in the majority of cases due to ill-defined boundaries or masking by fibrosis. We compared the mean area of active lesions to that of inactive lesions, excluding type 3 lesions with a very small area, and unclassified fibrotic lesions. The inactive lesions had a larger mean area than the active lesions, with respective values of 3.86 mm^2 and 2.92 mm^2.

4.5. Artifacts

Despite the many advantages of OCT-A, concerns are arising relating to its high susceptibility to artifacts that are important to recognize for a good interpretation [37].OCT-A image acquisition is based on the movement of blood flow within static tissue structures attested by successive B-scans at the same location. Thus, an impeccable fixation, frequently impaired in AMD, is a necessary condition, and any patient movement or eye movement during the acquisition may generate artifacts on the OCT-Angiograms [27]. The "Eye-tracking" technology was introduced to reduce these motion artifacts. By detecting and correcting the eye movements in real time, it provides better image quality at the cost of longer acquisition time [38]. All OCT-A prototypes currently available are equipped with eye-tracking technology, including the SS-OCT-A prototype used in our study. The movements of blood cells in the superficial retinal vessels cast fluctuating shadows on the deepest structures, sometimes mistaken for a real flow generating a false positive image of neovascular complex named a "projection artifact" [39]. A classic example of a projection artifact is the visualization of retinal vessels at the level of the RPE on the en face OCT-Angiograms. Posterior shadowing artifacts reported in our study were essentially due to subretinal fibrosis and drusen.

Distortion of the different retinal layers is frequently associated with MNV and exudative signs and can cause segmentation artifacts, as automatic segmentation algorithms are generated from healthy eyes. Several OCT-A prototypes are equipped with a software allowing manual correction of segmentation on the cross-sectional images. In our study, we used the automated segmentation only.

4.6. Study limitations

AMD is a pathology of the elderly. The number of cases included in our study was limited mainly because of the lack of cooperation of some patients when OCT-A was being performed. On the other hand, our study being cross-sectional, the evolution of MNV was not examined. Thus, it was impossible for us to analyze the contribution of OCT-A in long-term monitoring of MNV in wet AMD. On the technical side, The device detects the decorrelation signal only if the vascular flow is above a minimum threshold: A blood flow within the neovascular lesion lower than the minimum threshold would not be visualized. Segmentation errors and artifacts can also occur and have been detailed above. These technical limitations we are currently facing are being improved.

5. Conclusion

Recently introduced, OCT-A is a non-invasive, safe and reproducible retinal imaging technique. By segmenting the retina into different layers, it provides high-resolution angiographs facilitating the analysis of the microvascular abnormalities occurring in AMD. OCT-A demonstrated a high sensitivity of detection of MNV and made it possible to evaluate the presence vascular blood flow inside quiescent and fibrotic lesions. The lesion's feeder vessels is frequently identified using OCT-A while dye injection conventional techniques always fail its detection. The involvement of OCT-A in the treatment decision for MNV in AMD is linked to identifying the "pattern" of the lesion reflecting its active or inactive status. However, indicating an antiangiogenic treatment based on OCT-A alone can sometimes be quite challenging, especially for recurrent neovascular lesions. Comparing en face and cross-sectional OCT-Angiograms in order to indentify exudative signs could help assess the activity status of the lesion without recourse to conventional dye-injection imaging techniques. OCT-A should be performed first-line in the presence of any macular lesion suggestive of AMD in order to identify the neovascular complex and to assess its morphological characteristics. The absence of a neovascular network on OCT-A should lead to further investigations using conventional dye-injection imaging techniques in order to confirm or rule out the diagnosis. There are no contraindications for OCT-A, it's a totally safe imaging technique. In the future, OCT-A could provide new data correlating structural and functional parameters, allowing a better understanding of the pathophysiology of exudative AMD as well as its natural history, in order to propose personalized therapeutic approach.

Sources of funding

None.

Ethical approval

Written informed consent was obtained from each patient.
Our study was carried out in compliance with the Helsinki Declaration.

Consent

Patients' privacy was fully respected.
There are no identifying details in our study.

Author contribution

Study concept: MAHJOUB Ahmed.
Writing the paper: BEN MRAD Syrine, MAHJOUB Ahmed
Data collection: BEN MRAD Syrine, MAHJOUB Ahmed.
Contributors: BEN ABDESSLEM Nadia, MAHJOUB Anis, ZINELABIDINE Karim, GHORBEL Mohamed, MAHJOUB Hachemi, KRIFA Fethi, KNANI Leila.

Trial registry number

1. Name of the registry: OPTICAL COHERENCE TOMOGRAPHY ANGIOGRAPHY FEATURES OF MACULAR NEOVASCULARIZATION IN WET AGE-RELATED MACULAR DEGENERATION: A CROSS-SECTIONAL STUDY.
2. Unique Identifying number or registration ID: researchregistry7027.
3. Hyperlink to your specific registration (must be publicly accessible and will be checked): https://www.researchregistry.com/browse-the-registry#home/registrationdetails/610ad5ccc99ae6001e46fb7f/

Guarantor

MAHJOUB Ahmed.
BEN MRAD Syrine.

Declaration of competing interest

We declare that there is no conflict of interest.

Appendix A. Supplementary data

Supplementary data to this article can be found online at https://doi.org/10.1016/j.amsu.2021.102826.

References

[1] N.M. Bressler, Age-related macular degeneration is the leading cause of blindness, J. Am. Med. Assoc. 291 (2004) 1900–1901.
[2] W.L. Wong, X. Su, X. Li, et al., Global prevalence of age-related macular degeneration and disease burden projection for 2020 and 2040: a systematic review and meta-analysis, Lancet Glob. Health 2 (2) (2014) e106–e116.
[3] P. Mitchell, G. Liew, B. Gopinath, T.Y. Wong, Age-related macular degeneration, Lancet 392 (10153) (2018) 1147–1159.
[4] F. Sulzbacher, C. Kiss, M. Munk, et al., Diagnostic evaluation oftype 2 (classic) choroidal neovascularization: optical coherence tomography, indocyanine green angiography, and fluorescein angiography, Am. J. Ophthalmol. 152 (5) (2011) 799–806.
[5] P.E. Stanga, J.I. Lim, P. Hamilton, Indocyanine green angiography in chorioretinal diseases: indications and interpretation:an evidence-based update, Ophthalmology 110 (2003) 15–21.
[6] Y. Jia, O. Tan, J. Tokayer, et al., Split-spectrum amplitude decorrelation angiography with optical coherence tomography, Opt Express 20 (4) (2012) 4710–4725.
[7] M. Lupidi, A. Cerquaglia, J. Chhablani, et al., Optical coherence tomography angiography in age-related macular degeneration: the game changer, Eur. J. Ophthalmol. 28 (4) (2018) 349–357.
[8] R. Agha, A. Abdall-Razak, E. Crossley, N. Dowlut, C. Iosifidis, G. Mathew, for the STROCSS Group, The STROCSS 2019 guideline: strengthening the reporting of cohort studies in surgery, Int. J. Surg. 72 (2019) 156–165.
[9] R.F. Spaide, G.J. Jaffe, D. Sarraf, K.B. Freund, S.R. Sadda, G. Staurenghi, N. K. Waheed, U. Chakravarthy, P.J. Rosenfeld, F.G. Holz, E.H. Souied, S.Y. Cohen, G. Querques, K. Ohno-Matsui, D. Boyer, A. Gaudric, B. Blodi, C.R. Baumal, X. Li, G. J. Coscas, A. Brucker, L. Singerman, P. Luthert, S. Schmitz-Valckenberg, U. Schmidt-Erfurth, H.E. Grossniklaus, D.J. Wilson, R. Guymer, L.A. Yannuzzi, E. Y. Chew, K. Csaky, J.M. Monés, D. Pauleikhoff, R. Tadayoni, J. Fujimoto, Consensus nomenclature for reporting neovascular age-related macular degeneration data: consensus on neovascular age-related macular degeneration nomenclature study group, Ophthalmology 127 (5) (2020 May) 616–636.
[10] G.J. Coscas, M. Lupidi, F. Coscas, C. Cagini, E.H. Souied, Optical coherence tomography angiography versus traditional multimodal imaging in assessing the activity of exudative age-related macular degeneration: a New Diagnostic Challenge, Retina 35 (11) (2015) 2219–2228.
[11] R.F. Spaide, G.J. Jaffe, D. Sarraf, et al., Consensus nomenclature for reporting neovascular age-related macular degeneration data: consensus on neovascular age-related macular degeneration nomenclature study group, Ophthalmology 127 (5) (2020) 616–636.
[12] J.D. Gass, Pathogenesis of disciform detachment of the neuroepithelium, Am. J. Ophthalmol. 63 (3) (1967) 1–139.
[13] A. Faridi, Y. Jia, S.S. Gao, D. Huang, K.V. Bhavsar, D.J. Wilson, et al., Sensitivity and specificity of OCT angiography to detect choroidal neovascularization, Ophthalmol. Retin. 1 (2017) 294–303.
[14] D. Ahmed, M. Stattin, A. Graf, J. Forster, C. Glittenberg, I. Krebs, S. Ansari-Shahrezaei, Detection of treatment-naive choroidal neovascularization in age-related macular degeneration by swept source optical coherence tomography angiography, Retina 38 (11) (2018) 2143–2149.

[15] J.H. Yeo, H. Chung, J.T. Kim, Swept-source optical coherence tomography angiography according to the type of choroidal neovascularization, J. Clin. Med. 8 (9) (2019) 1272.

[16] F. Coscas, D. Cabral, T. Pereira, C. Geraldes, H. Narotamo, A. Miere, M. Lupidi, A. Sellam, A. Papoila, G. Coscas, E. Souied, Quantitative optical coherence tomography angiography biomarkers for neovascular age-related macular degeneration in remission, PloS One 13 (10) (2018), e0205513.

[17] L. Von der Emde, S. Thiele, M. Pfau, J. Nadal, J. Meyer, P.T. Möller, M. Schmid, M. Fleckenstein, F.G. Holz, S. Schmitz-Valckenberg, Assessment of exudative activity of choroidal neovascularization in age-related macular degeneration by OCT angiography, Ophthalmologica 243 (2) (2020) 120–128.

[18] M. Karacorlu, I. Sayman Muslubas, S. Arf, M. Hocaoglu, M.G. Ersoz, Membrane patterns in eyes with choroidal neovascularization on optical coherence tomography angiography, Eye 33 (8) (2019) 1280–1289.

[19] L. Kuehlewein, K.K. Dansingani, T.E. de Carlo, M.A. Bonini Filho, N.A. Iafe, T. L. Lenis, K.B. Freund, N.K. Waheed, J.S. Duker, S.R. Sadda, D. Sarraf, Optical coherence tomography angiography of type 3 neovascularization secondary to age-related macular degeneration, Retina 35 (11) (2015) 2229–2235.

[20] A. Miere, G. Querques, O. Semoun, F. Amoroso, O. Zambrowski, T. Chapron, et al., Optical coherence tomography angiography changes in early type 3 neovascularization after antivascular endothelial growth factor treatment, Retina 37 (10) (2017) 1873–1879.

[21] A. Kawamura, M. Yuzawa, R. Mori, M. Haruyama, K. Tanaka, Indocyanine green angiographic and optical coherence tomographic findings support classification of polypoidal choroidal vasculopathy into two types, Acta Ophthalmol. 91 (2013) e474–e481.

[22] L. Kuehlewein, M. Bansal, T.L. Lenis, N.A. Iafe, S.R. Sadda, Filho MA. Bonini, et al., Optical coherence tomography angiography of type 1 neovascularization in age related macular degeneration, Am. J. Ophthalmol. 160 (2015) 739–748.

[23] A. Carnevali, M.V. Cicinelli, V. Capuana, F. Corvi, A. Mazzaferro, L. Querques, et al., Optical coherence tomography angiography: a useful tool for diagnosis of treatment naïve quiescent choroidal neovascularization, Am. J. Ophthalmol. 169 (2016) 189–198.

[24] E.H. Souied, A. Miere, S.Y. Cohen, O. Semoun, G. Querques, Optical coherence tomography angiography of fibrosis in age-related macular degeneration, Dev. Ophthalmol. 56 (2016) 86–90.

[25] A. El Ameen, S.Y. Cohen, O. Semoun, A. Miere, M. Srour, M. Quaranta-El Maftouhi, H. Oubraham, R. Blanco-Garavito, G. Querques, E.H. Souied, Type 2 neovascularization secondary to age-related macular degeneration imaged by optical coherence tomography angiography, Retina 35 (11) (2015) 2212–2218.

[26] G. Querques, A. Miere, E.H. Souied, Optical coherence tomography angiography features of type 3 neovascularization in age-related macular degeneration, Dev. Ophthalmol. 56 (2016) 57–61.

[27] A. Miere, O. Semoun, S.Y. Cohen, A. El Ameen, M. Srour, C. Jung, H. Oubraham, G. Querques, E.H. Souied, Optical coherence tomography angiography features of subretinal fibrosis in age-related macular degeneration, Retina 35 (11) (2015) 2275–2284.

[28] M. Al-Sheikh, N.A. Iafe, N. Phasukkijwatana, S.R. Sadda, D. Sarraf, Biomarkers of neovascular in age-related macular degeneration using optical coherence tomography angiography, Retina 38 (2) (2018) 220–230.

[29] F. Sulzbacher, A. Pollreisz, A. Kaider, S. Kickinger, S. Sacu, U. SchmidtErfurth, On behalf of the Vienna Eye Study Center. Identification and clinical role of choroidal neovascularization characteristics based on optical coherence tomography angiography, Acta Ophthalmol. 95 (2017) 414–420.

[30] L. Solecki, P. Loganadane, A.S. Gauthier, M. Simonin, M. Puyraveau, B. Delbosc, M. Saleh, Predictive factors for exudation of quiescent choroidal neovessels detected by OCT angiography in the fellow eyes of eyes treated for a neovascular age-related macular degeneration, Eye (Lond.) 35 (2) (2021 Feb) 644–650.

[31] R.F. Spaide, Optical coherence tomography angiography signs of vascular abnormalization with antiangiogenic therapy for choroidal neovascularization, Am. J. Ophthalmol. 160 (2015) 6–16.

[32] N.W. Muakkassa, A.T. Chin, T. de Carlo, K.A. Klein, C.R. Baumal, A.J. Witkin, J. S. Duker, N.K. Waheed, Characterizing the effect of anti-vascular endothelial growth factor therapy on treatment-naive choroidal neovascularization using optical coherence tomography angiography, Retina 35 (2015) 2252–2259.

[33] F. Coscas, M. Lupidi, J.F. Boulet, A. Sellam, D. Cabral, R. Serra, C. Français, E. H. Souied, G. Coscas, Optical coherence tomography angiography in exudative age-related macular degeneration: a predictive model for treatment decisions, Br. J. Ophthalmol. 103 (9) (2019) 1342–1346.

[34] E.H. Souied, A. El Ameen, O. Semoun, A. Miere, G. Querques, S.Y. Cohen, Optical coherence tomography angiography of type 2 neovascularization in age-related macular degeneration, Dev. Ophthalmol. 56 (2016) 52–56.

[35] Y. Jia, S.T. Bailey, D.J. Wilson, O. Tam, M.L. Klein, C.J. Flaxel, et al., Quantitative optical coherence tomography angiography of choroidal neovascularization in age related macular degeneration, Ophthalmology 121 (2014) 1435–1444.

[36] F. Amoroso, A. Miere, O. Semoun, C. Jung, V. Capuano, E.H. Souied, Optical coherence tomography angiography reproducibility of lesion size measurements in neovascular age-related macular degeneration (AMD), Br. J. Ophthalmol. 102 (6) (2018) 821–826.

[37] E.D. Cole, E.M. Moult, S. Dang, W. Choi, S.B. Ploner, B. Lee, R. Louzada, E. Novais, J. Schottenhamml, L. Husvogt, A. Maier, J.G. Fujimoto, N.K. Waheed, J.S. Duker, The definition, rationale, and effects of thresholding in OCT angiography, Ophthalmol. Retina 1 (5) (2017) 435–447.

[38] J.L. Lauermann, M. Treder, P. Heiduschka, C.R. Clemens, N. Eter, F. Alten, Impact of eye-tracking technology on OCT-angiography imaging quality in age-related macular degeneration, Graefes Arch. Clin. Exp. Ophthalmol. 255 (8) (2017) 1535–1542.

[39] F. Zheng, L. Roisman, K.B. Schaal, A.R. Miller, G. Robbins, G. Gregori, P. J. Rosenfeld, Artifactual flow signals within drusen detected by OCT angiography, Ophthal. Surg. Lasers Imag. Retina 47 (6) (2016) 517–522.